INSTITUTE OF PHYSICS PUBLISHING JOURNAL OF PHYSICS: CONDENSED MATTER

J. Phys.: Condens. Matter **17** (2005) S2089–S2098 doi:10.1088/0953-8984/17/21/005

Modelling of dielectric constants of amorphous Zr silicates

G-M Rignanese[1,2] **and Alfredo Pasquarello**[3,4]

[1] Unité de Physico-Chimie et de Physique des Matériaux, Université Catholique de Louvain, 1 Place Croix du Sud, B-1348 Louvain-la-Neuve, Belgium
[2] Research Center on Microscopic and Nanoscopic Materials and Electronic Devices (CERMIN), Université Catholique de Louvain, B-1348 Louvain-la-Neuve, Belgium
[3] Ecole Polytechnique Fédérale de Lausanne (EPFL), Institute of Theoretical Physics, CH-1015 Lausanne, Switzerland
[4] Institut Romand de Recherche Numérique en Physique des Matériaux (IRRMA), CH-1015 Lausanne, Switzerland

E-mail: rignanese@pcpm.ucl.ac.be

Received 3 January 2005, in final form 1 March 2005
Published 13 May 2005
Online at stacks.iop.org/JPhysCM/17/S2089

Abstract

We discuss various decomposition schemes for analysing the dielectric constants of Zr silicates in terms of local properties. Such schemes serve the purpose of predicting the dielectric constants of amorphous alloys, when their system size precludes the possibility of performing accurate first-principles calculations. In particular, we compare two decomposition schemes which have found application in the recent literature. The first scheme is based on a decomposition into basic structural units characterized by effective parameters. While this scheme was originally developed for cation-centred structural units, we here also consider its application to anion-centred structural units. In the second scheme, the difference between the static and optical dielectric constants is formally decomposed into atomic contributions. We analyse the results of these two schemes when applied to a set of $(ZrO_2)_x(SiO_2)_{1-x}$ model structures, for which the dielectric properties are computed from first principles. The most promising results are recorded for the first scheme when applied to cation-centred structural units.

1. Introduction

As CMOS devices are built with smaller and smaller features, the scaling laws for their operation impose continuous reductions of the thickness of the silicon dioxide gate. The current International Technology Roadmap for Semiconductors projects that the SiO_2 layer at the gate electrode will be only 7 Å thick by 2012 [1]. At this scale, the oxide consists of only

a few atomic layers and direct tunnelling of electrons through the oxide significantly increases the leakage current, thereby impairing the device performance.

In order to avoid this materials limit, the microelectronics industry has intensively been searching for alternative gate materials of high permittivity (κ). The increase of the dielectric constant compared to SiO_2 allows the use of gates with larger physical thicknesses (t_{phys}), while preserving the same capacitance as SiO_2 gates of smaller thickness (t_{ox}):

$$t_{\mathrm{ox}} = \frac{\kappa_{\mathrm{ox}}}{\kappa} t_{\mathrm{phys}},$$

κ_{ox} being the dielectric constant of SiO_2. The larger physical thickness solves the leakage problems, as well as other problems resulting from the penetration of the gate dopants in the substrate. However, replacing the SiO_2 is not as simple as it may seem. Indeed, besides showing a high dielectric constant, a potential high-κ replacement must satisfy many stringent requirements, such as the thermodynamic stability with the Si interface or the high level interface quality.

The leading candidates for meeting these criteria are the silicates of hafnium and zirconium in the form of amorphous films. The dielectric properties of these materials have therefore been studied quite intensively. Early experimental measurements tend to show a superlinear dependence of the static dielectric constant κ_0 on the Hf/Zr concentration [2, 3]. This behaviour has been addressed by several phenomenological theories [4, 5]. However, a close to linear dependence has emerged from more recent experiments [6, 7]. The latter dependence has found support in a recent theoretical analysis based on first-principles calculations [8].

First-principles calculations based on density-functional theory (DFT) indeed constitute a valuable tool for understanding the properties of materials at the atomic scale. In particular, these calculations have demonstrated a high predictive power as far as the dielectric properties are concerned. This makes these calculations particularly useful when the experimental situation is unclear. However, in this particular field, one faces the general issue of predicting the dielectric properties of *amorphous* alloys. Brute force calculations of numerous large supercells are at present beyond the reach of first-principles methods. Therefore, it is necessary to devise viable schemes for extending first-principles results achieved on selected model structures to the case of large disordered structures.

We have recently introduced such a scheme by relating the dielectric constants to the local bonding of Si and Hf/Zr atoms [8]. This scheme is based on a decomposition into cation-centred structural units, characterized by a set of effective parameters. In a subsequent study on amorphous ZrO_2 [9], Zhao, Cersoli and Vanderbilt proposed a different analysis, in which the lattice contribution to the dielectric constant is decomposed into atomic parts. Applied to amorphous Zr silicates, the first scheme has been found to provide a good description of both the optical and static dielectric constants [8]. The second scheme offers the advantage of a formally exact decomposition, but its usefulness for predicting dielectric constants has so far not been addressed.

In this paper, we compare various available schemes leading to analyses of dielectric constants in terms of local properties. In particular, we carry out decompositions into contributions pertaining to structural units and to atoms. We also consider variants in which either the anions or the cations assume the central role. The ultimate aim is to identify the most promising scheme for predicting the dielectric properties of amorphous Zr silicates.

2. Technical details

All our calculations are performed using the ABINIT package [10]. The exchange–correlation energy is evaluated within the local density approximation (LDA) to DFT, using Perdew–Wang's parametrization [11] of Ceperley–Alder electron-gas data [12].

Table 1. Description of the various model structures in terms of cation-centred and anion-centred structural units. The symbols indicated between parentheses refer to figures 2 and 3.

Model	Cation-centred SUs	Anion-centred SUs
C_0 (○)	4 SiO_4	8 OSi_2
C_1 (□)	3 SiO_4 + 1 ZrO_4	4 OSi_2 + 4 OSiZr
Q_0 (●)	3 SiO_4	6 OSi_2
Q_1 (■)	2 SiO_4 + 1 ZrO_4	2 OSi_2 + 4 OSiZr
S_0 (●)	2 SiO_6	4 OSi_3
S_1 (■)	1 SiO_6 + 1 ZrO_6	2 OSi_2Zr + 4 $OSiZr_2$
Z_0 (⊙)	2 SiO_4 + 2 SiO_6	4 OSi_2 + 4 OSi_3
Z_1 (▣)	2 SiO_4 + 1 SiO_6 + 1 ZrO_8	2 OSiZr + 6 OSi_2Zr
Z_2 (△)	2 SiO_4 + 2 ZrO_8	8 $OSiZr_2$
A (♦)	17 SiO_4 + 1 ZrO_7 + 2 ZrO_6	26 OSi_2 + 7 OSiZr + 2 OSi_2Zr + 5 $OSiZr_2$

Only valence electrons are explicitly considered using pseudopotentials to account for core–valence interactions. We use norm-conserving pseudopotentials [13] with Zr(4s, 4p, 4d, 5s), Si(3s, 3p), and O(2s, 2p) levels treated as valence states. The pseudopotentials are generated using the following atomic valence configurations: $Zr(4s^24p^64d^25s^0)$, $Si(3s^23p^2)$, and $O(2s^22p^4)$. In the case of Zr, we take core radii of 1.75, 1.55, and 1.70 au for describing angular waves from s to d. For the Si pseudopotential, the same cut-off radius of 2.00 au is used for the three lowest angular momentum waves. For the O pseudopotential, we use a cut-off radius of 1.50 au for both s and p waves. We adopt a separable form for the pseudopotentials [14] treating the following angular momentum waves as local: d for Zr, d for Si, and p for O. The wavefunctions are expanded in plane waves up to a kinetic energy cut-off of 30 Ha. The chosen kinetic energy cut-off and k-point sampling of the Brillouin zone ensure convergence of all the calculated properties.

In this work, we use the same model structures of $(ZrO_2)_x(SiO_2)_{1-x}$ as introduced previously [8]. These model structures, nine crystalline and one amorphous, show different Zr contents with x ranging from 0 to 0.5. For the convenience of the reader, we here summarize their salient features. The set includes three different SiO_2 polymorphs ($x = 0$): $[C_0]$ α-cristobalite, $[Q_0]$ α-quartz, and $[S_0]$ stishovite. Substitution of one of the Si atoms by a Zr atom in each of these models gives three new crystal structures: $[C_1]$ Zr^{Si} in α-cristobalite ($x = 0.25$), $[Q_1]$ Zr^{Si} in α-quartz ($x = 0.33$), $[S_1]$ Zr^{Si} in stishovite ($x = 0.5$). The other crystalline structures are obtained from $[Z_2]$ zircon. The replacement of Zr by Si gives $[Z_1]$ Si^{Zr} for one substitution per unit cell ($x = 0.25$), and $[Z_0]$ for fully Si-substituted zircon ($x = 0$). The amorphous structure $[A]$ corresponds to a periodically repeated cubic model containing 3 Zr, 17 Si, and 20 O atoms ($x = 0.15$) at a fixed density of 3.12 g cm^{-3} [15]. All the Si atoms are fourfold coordinated and the Zr atoms show an average coordination of 6.3, in accord with experimental data [4]. We refer to [8] for a detailed description of the generation procedure.

Apart from the amount of Zr incorporated in the silica (x), the different structures differ by the coordination of the atomic species Zr, Si, and O. This appears very clearly when describing the various structures in terms of cation-centred (CC) or anion-centred (AC) structural units (SUs). In a recent paper [8], we considered cation-centred structural units, which were centred on Si or Zr atoms and included the nearest-neighbour O atoms. Here, we also consider the alternative standpoint in which the SUs are centred on O atoms and include their nearest-neighbour Si and Zr atoms. The description of the various model structures in terms of both CC and AC structural units is provided in table 1.

The atomic coordinates and the cell parameters of all our model structures are fully relaxed within our first-principles approach. The corresponding dynamical and dielectric

Table 2. Composition (x), optical (ϵ_∞) and static (ϵ_0) dielectric constants, volume ($\bar{V}$) in bohr^3, polarizabilities $\bar{\alpha}_\infty$ and $\bar{\alpha}_0$ in bohr^3, characteristic dynamical charge ($\bar{Z}$), and characteristic force constant ($\bar{C}$) in hartree/bohr^2 for the various model systems.

Model	x	ϵ_∞	ϵ_0	$\bar{V}$	$\bar{\alpha}_\infty$	$\bar{\alpha}_0$	$\bar{Z}$	$\bar{C}$
C_0	0.00	2.38	4.30	264.77	19.92	33.11	4.21	0.4391
C_1	0.25	2.76	5.25	273.21	24.12	38.23	4.59	0.3895
Q_0	0.00	2.54	4.83	240.34	19.46	32.17	4.28	0.4169
Q_1	0.33	2.91	5.84	275.28	25.56	40.57	4.85	0.3661
S_0	0.00	3.36	10.33	153.74	16.16	27.77	4.81	0.2716
S_1	0.50	4.44	24.20	201.88	25.74	42.68	6.14	0.1188
Z_0	0.00	3.37	10.11	167.80	17.68	30.14	4.76	0.2512
Z_1	0.25	3.94	18.36	189.74	22.42	38.62	5.29	0.1287
Z_2	0.50	4.13	11.81	213.28	26.00	39.86	5.58	0.2385
A	0.15	3.24	8.92	213.12	21.75	36.30	4.83	0.2424

properties are computed within a variational approach to density-functional perturbation theory, as implemented in the ABINIT package [10]. This method is presented in detail in [16] and [17]. We adopt here the same notations as in these references. In particular, κ and α run over the atoms in the unit cell and over the three Cartesian directions, respectively.

The key quantities to be calculated are second-order derivatives of the energy. For obtaining the phonon frequencies and the related eigendisplacements $U_m(\kappa\alpha)$, we consider second derivatives with respect to collective atomic displacements. The second derivatives with respect to the macroscopic electric field give us access to the optical dielectric tensor $\epsilon^\infty_{\alpha\beta}$. The Born effective charge tensors $Z^*_{\kappa,\alpha\beta}$ [17] are obtained by considering mixed second derivatives with respect to the electric field and the atomic displacements. The static dielectric constant $\epsilon^0_{\alpha\beta}$ is obtained from

$$\epsilon^0_{\alpha\beta} = \epsilon^\infty_{\alpha\beta} + \frac{4\pi}{\Omega_0} \sum_m \frac{S_{m,\alpha\beta}}{\omega_m^2}. \tag{1}$$

where the mode-oscillator strength $S_{m,\alpha\beta}$ is defined as

$$S_{m,\alpha\beta} = \left(\sum_{\kappa\alpha'} Z^*_{\kappa,\alpha\alpha'} U^*_{m\mathbf{q}=\mathbf{0}}(\kappa\alpha') \right) \left(\sum_{\kappa'\beta'} Z^*_{\kappa',\beta\beta'} U_{m\mathbf{q}=\mathbf{0}}(\kappa'\beta') \right). \tag{2}$$

The optical and static dielectric constants[5] calculated for our model structures are given in table 2. Due to the well known limitations of the LDA, the theoretical values are larger than the experimental ones (when available) by about 10%.

3. Modelling of dielectric constants

The crudest scheme for modelling dielectric constants consists in assuming that these can be obtained from a sum of local quantities associated with structural units:

$$\epsilon = \sum_i x_i \epsilon_i, \tag{3}$$

where ϵ_i is the dielectric constant (either optical or static) and x_i is the molecular fraction for each SU i. The structural units can be either cation centred, in which case $i \equiv \mathrm{SiO}_n$ (with $n = 4$ or 6) or ZrO_n (with $n = 4$, 6, or 8), or anion centred, in which case $i \equiv \mathrm{OSi}_n$ (with

[5] Orientational averages are given.

Table 3. Characteristic parameters of cation-centred and anion-centred structural units obtained using the unphysical, the physical, and the alternative schemes: optical dielectric constant (ϵ_∞), difference between static and optical dielectric constants ($\Delta\epsilon$), polarizabilities (α_∞ and α_0 in bohr^3), charge (Z), and force constant (C in hartree/bohr^2).

CC SUs	Scheme		SiO_4	SiO_6	ZrO_4	ZrO_6	ZrO_8
	Unph.	ϵ_∞	2.56	3.58	3.51	5.30	5.97
		$\Delta\epsilon$	3.02	8.88	2.07	30.64	18.42
	Phys.	α_∞	19.68	16.14	37.37	35.35	32.69
		Z	4.29	4.92	5.66	7.16	6.73
		C	0.3597	0.2176	0.4202	0.0817	0.1153
	Alt.	α_0	32.85	28.25	55.43	57.10	49.60
AC SUs	Scheme		OSi_2	OSi_3	OSiZr	OSi_2 Zr	$OSiZr_2$
	Unph.	ϵ_∞	2.55	3.53	3.01	4.38	4.20
		$\Delta\epsilon$	2.68	7.74	1.85	22.08	9.63
	Phys.	α_∞	19.72	16.06	28.14	21.82	26.73
		Z	4.31	4.89	4.91	5.76	5.77
		C	0.3917	0.2483	0.3978	0.0967	0.2149
	Alt.	α_0	32.73	27.73	43.62	39.20	41.12

$n = 2$ or 3), OSiZr, OSi_2Zr, or $OSiZr_2$. Note that a similar relation can be defined for the difference between the static and optical dielectric constants ($\Delta\epsilon$):

$$\Delta\epsilon = \epsilon_0 - \epsilon_\infty = \sum_i x_i \Delta\epsilon_i . \tag{4}$$

Equations (3) and (4) do not rely on any physical argument. Worse, the dielectric constants are intensive quantities, hence not additive. Therefore, hereafter we will refer to this approach as to the *unphysical* scheme.

In the following, we consider equation (3) for the optical dielectric constant, whereas we prefer to work with equation (4) for the static dielectric constant. The optimal values for ϵ_i^∞ and $\Delta\epsilon_i$ for the various structural units are reported in table 3. They are obtained by solving in a least square sense the over-determined system based on the first-principles values of ϵ_∞ and $\Delta\epsilon$ for the nine crystalline models (table 2).

By introducing the values of ϵ_i^∞ and $\Delta\epsilon_i$ from table 3 in equations (3) and (4), the dielectric constants ϵ_∞ and $\Delta\epsilon$ can be obtained and compared with the first-principles results. The relative errors on ϵ_∞ and $\Delta\epsilon$ are reported in figure 1. These errors are found to be quite large irrespective of the choice of cation- and anion-centred structural units. This is a clear consequence of the unphysical character of this scheme. The smallest relative errors are found for ϵ_∞: they are of the order of 5% for the nine crystalline models, and of 10% for the amorphous model. For $\Delta\epsilon$, the error is about 20% for both crystalline and amorphous models.

To go beyond this crude approach, we have recently introduced a more physical scheme to relate the dielectric constants to the underlying atomic structure [8]. We refer to this approach as to the *physical* scheme. It consists in determining quantities that can be considered local and additive and from which ϵ_∞ and $\Delta\epsilon$ can be obtained.

For the optical dielectric constant, we use the Clausius–Mossotti relation [5, 7] to establish a link with the electronic polarizability $\bar{\alpha}_\infty$:

$$\frac{\epsilon_\infty - 1}{\epsilon_\infty + 2} = \frac{4\pi}{3}\frac{\bar{\alpha}_\infty}{\bar{V}} \tag{5}$$

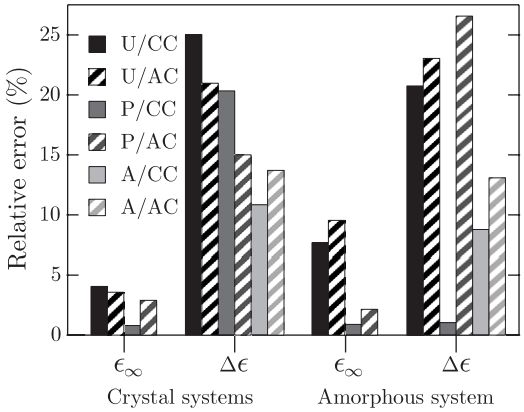

Figure 1. Relative errors on ϵ_∞ and $\Delta\epsilon$ obtained when using the unphysical [U] (in black), the physical [P] (in dark grey), and the alternative [A] (in light grey) schemes on the basis of a description of the model structures in terms of cation-centred [CC] (solid bars) or anion-centred [AC] (hatched bars) structural units. For the crystal systems, the reported errors correspond to an average over the nine models.

where $\bar{V}$ is the average SU volume. We then assume that

$$\bar{\alpha}_\infty = \sum_i x_i \alpha_i^\infty. \tag{6}$$

For the difference between the static and optical dielectric constants, the phonon contributions preclude a description in terms of a single local and additive quantity. We find it convenient to express $\Delta\epsilon$ as

$$\Delta\epsilon = \frac{4\pi}{\Omega_0} \sum_m \frac{S_m}{\omega_m^2} = \frac{4\pi}{\bar{V}} \frac{\bar{Z}^2}{\bar{C}}, \tag{7}$$

where ω_m and S_m are the frequency and the oscillator strength of the vibrational mode m. The volume of the primitive unit cell Ω_0 is related to the volume $\bar{V}$ and to the number of SUs $\bar{N}$ by $\Omega_0 = \bar{N}\bar{V}$. The characteristic dynamical charge $\bar{Z}$ and the characteristic force constant $\bar{C}$ are defined by $\bar{Z}^2 = (\sum_\kappa Z_\kappa^2)/\bar{N}$ and $\bar{C}^{-1} = (\sum_m S_m/\omega_m^2/\bar{Z}^2)/\bar{N}$, where Z_κ are the atomic Born effective charges. By analogy with the polarizability, we define Z_i and C_i values for each SU such that

$$\bar{Z}^2 = \sum_i x_i Z_i^2, \qquad \text{and} \qquad \bar{C}^{-1} = \sum_i x_i C_i^{-1}, \tag{8}$$

though the locality and the additivity of these parameters is not guaranteed *a priori*.

Alternatively to equations (7) and (8), the Clausius–Mossotti relation can also be used with the static dielectric constant [5] to define the ionic polarizability $\bar{\alpha}_0$,

$$\frac{\epsilon_0 - 1}{\epsilon_0 + 2} = \frac{4\pi}{3} \frac{\bar{\alpha}_0}{\bar{V}}, \tag{9}$$

which is assumed to be additive:

$$\bar{\alpha}_0 = \sum_i x_i \alpha_i^0. \tag{10}$$

The approach based on equations (5), (6), (9), and (10) will be referred to as the *alternative* scheme.

The optimal values for the parameters α_i^{∞}, α_i^{0}, Z_i, and C_i associated with the various structural units are reported in table 3. They are obtained by solving in a least square sense the three overdetermined systems based on the first-principles values of $\bar{\alpha}_{\infty}$, $\bar{\alpha}_0$, $\bar{Z}$, and $\bar{C}$ for the nine crystalline models. These first-principles values are reported in table 2.

Using equations (5), (6), (7) and (8) (or alternatively (5), (6), (9) and (10)) with the parameters of table 3, we calculate approximate values for ϵ_{∞} and ϵ_0. The relative errors on ϵ_{∞} and ϵ_0 with respect to the first-principles results are reported in figure 1. While the relative errors do not depend significantly on the description that is adopted (cation-centred or anion-centred SUs) within the unphysical and alternative schemes, this choice has a crucial effect within the physical scheme. First, for the crystalline systems, the relative error on ϵ_{∞} is less than 1% when adopting the description in terms of cation-centred SUs, whereas it becomes roughly three times larger with the description based on anion-centred SUs. The relative error on $\Delta\epsilon$ is large in both cases (see discussion below); it is actually slightly larger for the description in terms of CC structural units (20% compared to 15% with the AC structural units). Second, for the amorphous system, the difference is very pronounced, particularly for $\Delta\epsilon$. A description in terms of CC structural units gives relative errors of about 1% for both ϵ_{∞} and $\Delta\epsilon$. By contrast, the description based on AC structural units gives relative errors of $\sim$3% for ϵ_{∞} and of more than 25% for $\Delta\epsilon$.

The comparison for the amorphous system is particularly meaningful, since this structure was not used for determining the optimal values of the parameters for the various SUs. It is clear that the physical scheme with a description in terms of CC structurals provides the best results by far. The alternative scheme provides better results for the crystalline systems but for the amorphous model the relative errors are about 10%.

A careful analysis of the physical scheme reveals that the errors mainly originate from the estimation of $\bar{C}$. For the crystalline systems, the descriptions in terms of CC and AC structural units lead to average relative errors of less than 2% and 3% for $\bar{Z}$, whereas we find the relative errors are 18% and 10% for $\bar{C}$. *A posteriori*, $\bar{C}$ appears to be less local and additive than $\bar{Z}$. In fact, the locality of $\bar{C}$ is closely related to the dynamical charge neutrality of the SUs. The most important contributions to $\bar{C}$ arise from infrared active modes of low frequency. To the extent that the dynamical charge carried by the SUs vanishes, long-range vibrations in which the SUs move as rigid units will be infrared inactive and the dominating contributions to $\bar{C}$ will come from rather localized distortive vibrations. Therefore, the closer the SUs are to dynamical charge neutrality, the more local $\bar{C}$, and the more valid the physical scheme.

In figure 2, we report the relative effective charge of both the cation-centred and anion-centred SUs as a function of the cation charge. The anionic charge of CC structural units is defined as the sum of the effective charges of its O atoms weighted by the inverse of the number of SUs to which the O atom belongs. The cationic charges of AC structural units are defined similarly. The relative charge of the SUs is the total charge expressed relatively to the cationic charge: it is positive when the cationic charge is larger than the anionic charge, and vice versa. In figure 2, the data points referring to CC and AC structural units fall in distinct regions because of the different cation charge carried by the SUs in the two alternative descriptions. CC structural units carry a cation charge corresponding to that of its central atom, whereas AC structural units show cationic charges which roughly correspond to the negative of the charge carried by the central oxygen atom. In figure 2, the dispersion of the relative charge for the crystalline models is very similar for both CC and AC structural units. However, for the amorphous system, the CC structural units clearly appear to be more neutral. This explains why the physical scheme works better with cation-centred SUs.

It is interesting to note the dynamical charge neutrality of cation-centred SUs has also been found to be well respected in disordered silica [18]. We expect that the physical scheme based

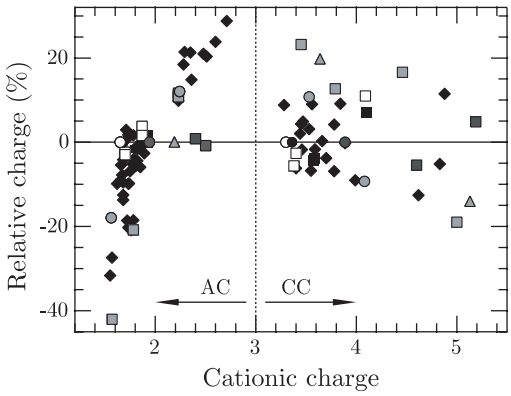

Figure 2. Relative charge of the structural units as a function of their cationic charge (see text) for the various model structures. The cation-centred and anion-centred SUs are on the right-hand and left-hand side of the graph, respectively, as indicated by the arrows and the vertical separation line. The symbols are those of table 1.

on a description in terms of CC structural units should be very effective in a variety of oxide glasses. Applied to amorphous $(ZrO_2)_x(SiO_2)_{1-x}$, this scheme has been found to successfully describe the observed dependence of the dielectric constants on the Zr concentration [8].

In a recent paper [9], a different decomposition scheme for dielectric constants has been proposed in the context of a study on amorphous ZrO_2. This scheme consists in a formally exact decomposition of the difference between ϵ_0 and ϵ_∞ into atomic parts. By combining equation (1) and (2) and changing the order of the summations, $\Delta\epsilon$ can first be decomposed into contributions from pairs of atoms κ and κ':

$$\Delta\epsilon_{\alpha\beta} = \sum_{\kappa\kappa'} \frac{1}{N^2} \Delta\epsilon_{\alpha\beta}^{\kappa\kappa'} \qquad \text{with } \Delta\epsilon_{\alpha\beta}^{\kappa\kappa'} = \frac{4\pi N^2}{\Omega_0} \sum_m \frac{(R_{m,\alpha}^{\kappa})^* R_{m,\beta}^{\kappa'}}{\omega_m^2} \tag{11}$$

where

$$R_{m,\alpha}^{\kappa} = \sum_{\alpha'} Z_{\kappa,\alpha\alpha'}^* U_{m\mathbf{q}=\mathbf{0}}(\kappa\alpha'). \tag{12}$$

With respect to the original scheme of [9], we have introduced the number of atoms per unit cell N in order to make of $\Delta\epsilon_{\alpha\beta}^{\kappa\kappa'}$ an intensive quantity. The contribution associated with a given atom κ can then be heuristically defined as

$$\Delta\epsilon_{\alpha\beta}^{\kappa} = \sum_{\kappa'} \tfrac{1}{2}(\Delta\epsilon_{\alpha\beta}^{\kappa\kappa'} + \Delta\epsilon_{\alpha\beta}^{\kappa'\kappa}), \tag{13}$$

so that

$$\Delta\epsilon_{\alpha\beta} = \sum_{\kappa} \frac{1}{N} \Delta\epsilon_{\alpha\beta}^{\kappa}, \tag{14}$$

where $\Delta\epsilon_{\alpha\beta}^{\kappa}$ is again an intensive quantity.

In figure 3, we report the calculated atomic contributions[6] for the various model structures. For a given atomic species, we distinguish between several bonding environments. The absolute scales for the various species and bonding environments can differ by as much as an order of magnitude. For clarity, the various contributions in figure 3 are therefore represented with respect to the maximal contribution obtained for each atomic species in a given bonding environment.

[6] Orientational averages are given.

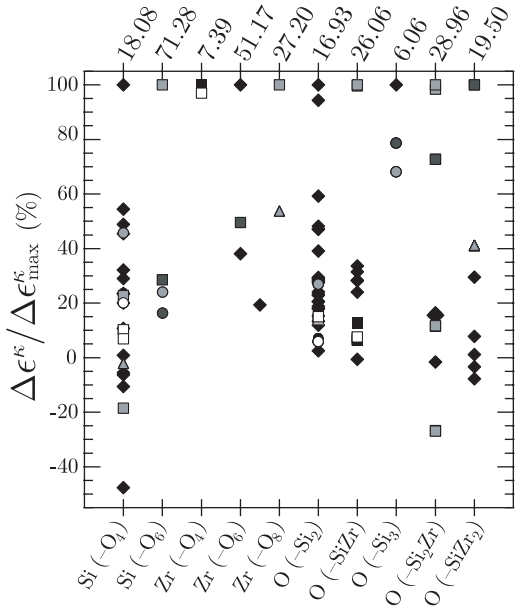

Figure 3. Atomic contributions to the static dielectric constant for the various model structures. The contributions are reported relative to the maximal contribution yielded for each atomic species in a given bonding environment (indicated at the top of the figure). The data point located in between $Zr(-O_6)$ and $Zr(-O_8)$ corresponds to a sevenfold coordinated Zr atom in the amorphous model; its contribution is expressed relatively to the maximal contribution of $Zr(-O_6)$.

The data present a very large dispersion and it is quite difficult to extract useful information from figure 3. It can be seen that the largest absolute contribution originates from a $Si(-O_6)$ atom found in the Z_1 crystalline model, but the achieved value appears exceptional and is not matched by similarly bonded Zr atoms in other model structures. Nevertheless, the $Zr(-O_6)$ atoms show the largest average value. In particular, the $Zr(-O_6)$ atoms in the amorphous model are found to contribute significantly to the dielectric constant. Interestingly, when using the physical scheme, it was also found that the ZrO_6 units give the largest contribution to $\Delta\epsilon$ in amorphous Zr silicates [8]. The maximal contributions associated with the variously bonded O atoms present less variation than for the other species. However, no definite trend emerges from this analysis.

It is interesting to note that this scheme based on a decomposition into atomic parts can be related to the unphysical scheme introduced above. Indeed, once the atomic contributions to $\Delta\epsilon$ are calculated, it is straightforward to obtain the contribution of the different structural units by summing the contribution of the central atom and those of its nearest neighbours weighted by the inverse of the number of SUs to which those neighbours belong. Hence, after taking an orientational average, equation (14) becomes

$$\Delta\epsilon = \sum_i \frac{1}{\bar{N}} \Delta\epsilon_i \tag{15}$$

where the sum now runs over all the structural units. This formula is very similar to (4), apart from the fact that the SUs are considered on an individual basis rather than by type. The large dispersion found for the contributions associated with atomic species in given bonding environments persists when considering the corresponding SUs. This clearly explains the poor performance of the unphysical scheme, which assumes a unique value of $\Delta\epsilon$ for a given SU type.

4. Conclusion

In this paper, we discuss various schemes for decomposing dielectric constants of Zr silicates into partial contributions carrying a local character. In particular, we address two schemes which have appeared in the recent literature. The first scheme consists in identifying basic structural units characterized by effective parameters [8]. We here considered descriptions in terms of both cation- and anion-centred structural units. The second scheme [9] is based on a formally exact atomic decomposition of the difference between the static and optical dielectric constants.

We have shown that the physical scheme is very successful when adopting a description in terms of cation-centred structural units. In fact, the dynamical charge neutrality of the SUs is demonstrated to be the key of the success of this scheme. Therefore, we suggest that this scheme should carry a more general validity and be applicable to any oxide glass respecting the dynamical charge neutrality within the structural units.

The second decomposition scheme yields atomic contributions showing considerable dispersion, thereby undermining the possibility of deriving a scheme for predicting the dielectric constants of amorphous Zr silicates. Since the decomposition in this second scheme is exact, the observed dispersion provides a clear explanation for the failure of straightforward decomposition schemes. Applied to the amorphous model, the second scheme reveals that the most significant contributions to the dielectric constant come from sixfold coordinated Zr atoms. This result is in agreement with the analysis carried out with the first scheme, which also identified the ZrO_6 structural units as the major contributors.

Acknowledgments

G-MR is grateful to the National Fund for Scientific Research (FNRS). Parts of this work are also connected to the NanoQuanta and FAME European networks of excellence.

References

[1] http://public.itrs.net
[2] Wilk G D and Wallace R M 2000 *Appl. Phys. Lett.* **76** 112–4
[3] Wilk G D, Wallace R M and Anthony J M 2000 *J. Appl. Phys.* **87** 484–92
[4] Lucovsky G and Rayner G B J 2000 *Appl. Phys. Lett.* **77** 2912–4
[5] Kurtz H A and Devine R A B 2001 *Appl. Phys. Lett.* **79** 2342–4
[6] Qi W J, Nieh R, Dharmarajan E, Lee B H, Jeon Y, Kang L, Onishi K and Lee J C 2000 *Appl. Phys. Lett.* **77** 1704–6
[7] van Dover R B, Manchanda L, Green M L, Wilk G, Garfunkel E and Busch B 2001 unpublished
[8] Rignanese G M, Detraux F, Gonze X, Bongiorno A and Pasquarello A 2002 *Phys. Rev. Lett.* **89** 117601:1–4
[9] Zhao X, Ceresoli D and Vanderbilt D 2005 *Phys. Rev.* B **71** 085107:1–10
[10] Gonze X, Beuken J M, Caracas R, Detraux F, Fuchs M, Rignanese G M, Sindic L, Verstraete M, Zerah G, Jollet F, Torrent M, Roy A, Mikami M, Ghosez P, Raty J Y and Allan D C 2002 *Comput. Mater. Sci.* **25** 478–92 (http://www.abinit.org)
[11] Perdew J P and Wang Y 1992 *Phys. Rev.* B **45** 13244–9
[12] Ceperley D M and Alder B J 1980 *Phys. Rev. Lett.* **45** 566–9
[13] Teter M 1993 *Phys. Rev.* B **48** 5031–41
[14] Kleinman L and Bylander D M 1982 *Phys. Rev. Lett.* **48** 1425
[15] Nogami M 1985 *J. Non-Cryst. Solids* **69** 415–23
[16] Gonze X 1997 *Phys. Rev.* B **55** 10337–54
[17] Gonze X and Lee C 1997 *Phys. Rev.* B **55** 10355–68
[18] Pasquarello A and Car R 1997 *Phys. Rev. Lett.* **79** 1766–9